Journal of Power Sources 224 (2013) 241–249

Contents lists available at SciVerse ScienceDirect

Journal of Power Sources

journal homepage: www.elsevier.com/locate/jpowsour

Atomic ensemble effects on formic acid oxidation on PdAu electrode studied by first-principles calculations

D.W. Yuan*, Z.R. Liu

College of Materials Science and Engineering, Hunan University, Changsha 410082, China

HIGHLIGHTS

- First-principles calculations and NEB simulations for HCOOH's decomposition on PdAu(111) surfaces.
- Ensemble effects on formic acid oxidation on Pd-decorated Au(111) surface.
- H production from formic acid through the direct pathway on Pd-decorated Au(111) surface.

ARTICLE INFO

Article history:
Received 1 August 2012
Received in revised form
27 September 2012
Accepted 29 September 2012
Available online 9 October 2012

Keywords:
Formic acid oxidation
Palladium–gold surfaces
Ensemble effects
Catalytic reaction
First-principles calculation

ABSTRACT

Using first-principles methods, we investigated the reaction pathways of the formic acid oxidation on Pd(111) and PdAu(111) surfaces. The dehydrogenation of formic acid can simultaneously occur *via* C–H and O–H activation on different Pd ensembles. However, on the contiguous ensembles without threefold Pd hollow, the reaction of COOH → CO + OH proceeds with a high activation energy (~1.00 eV), and the direct pathway is predominant for H production from formic acid. Our results indicates that the proper arrangement of Au and Pd sites can significantly improve electrocatalytic activity of PdAu catalyst for formic acid oxidation attributed to the reduction of poisoning species of CO_{ad}.

1. Introduction

Formic acid is an ideal source of hydrogen for fuel cells, which is a feasible alternative energy devices in portable electronic appliances, such as cell phones, MP3 players, and laptop computers, since HCOOH can decompose at near room temperatures to produce H_2 on Pt-, Pd-, and Au-based catalysts [1–6]. Generally, the oxidation of formic acid on anodes follows the so-called dual pathways: [7]

direct pathway I: $HCOOH \rightarrow CO_2 + 2H^+ + 2e^-$;

indirect pathway II: $HCOOH \rightarrow CO_{ad} + 2H_2O$.

Reaction I is the main pathway in the direct formic acid fuel cell (DFAFC), and a reactive intermediate of $HCOO_{ad}$ is formed *via* O–H scission in this pathway. The decomposition of $HCOO_{ad}$ to CO_2 is the rate-determining step for the direct oxidation of formic acid. [7] The poisoning species of CO_{ad} formed in the pathway II is only re-oxidized to CO_2 at high potentials. Thus, it is very important to significantly enhance the reactivity of dehydrogenation of $HCOO_{ad}$ and rapidly reduce the population of CO_{ad} for optimizing anode catalysts of DFAFC.

Pt is the most employed catalysts for HCOOH decomposition as the anode of DFAFC. However, HCOOH oxidation always proceeds through both direct and indirect pathways on Pt catalysts, and the intermediate of CO_{ad} usually poison the Pt surface. Theoretical investigations also suggested that CO_2 can be directly formed from the adsorbed HCOOH on Pt(111) surface [8,9]. Importantly, the rate of conversion of formic acid to CO_2 can be significantly enhanced on bimetallic Pt-based catalysts by modifying the atomic arrangements and electronic properties of reactive sites. [2] Recent investigations showed that the oxidation of formic acid occurs mainly through the direct dehydrogenation pathway without significant formation of the adsorbed CO on Pt-modified Au catalysts [10–12].

* Corresponding author. Tel.: +86 731 88664119; fax: +86 731 88664010.
E-mail address: dwyuan@hnu.edu.cn (D.W. Yuan).

0378-7753/$ – see front matter © 2012 Elsevier B.V. All rights reserved.
http://dx.doi.org/10.1016/j.jpowsour.2012.09.113

It should be noted that Pd-based catalysts show higher activity than Pt-based catalysts, and the oxidation pathways and catalytic activity are strongly dependent on the size and morphology of Pd nanoparticles [13]. More recently, K. Tedsree et al. reported Ag–Pd core–shell nanocatalysts can significantly enhance the production of H_2 from formic acid at ambient temperature, which attributes to the modification of electronic structure of Pd layers by the heterometallic bond between the surface atoms and the substrates [3]. Highly active Au–Pd catalysts were also found for the oxidation of formic acid [14–16]. Particularly, J.W. Hong [14] found the catalytic activity of Au–Pd bimetallic nanocrystals is strongly dependent on the atomic distribution of nanoparticle's (111) facets, and the Pd site decorated by Au exhibits high catalytic activity and stability for formic acid oxidation.

As known, the activity and selectivity of bimetallic catalysts not only depend on the "ligand effects" that encompass influences of bonding, change transfer, and strain [17,18], but also strongly on the "ensemble effects" that describe the synergistic behavior of different constituents in specific arrangements [19,20]. It was reported that the small Pt ensembles containing several metal atoms incorporated into metal substrates (e.g., Au surfaces) show the optimum catalytic activity for the direct oxidation of formic acid and methanol [10,21,22]. Notably, Pd-decorated Au catalysts can markedly improve the catalytic efficiency toward vinyl acetate (VA) synthesis and CO oxidation through the pure "ensemble effects" [23–26]. In order to exploring a novel catalyst for enhancing the chemical activity of formic acid oxidation with a CO-free pathway, thus, it is imperative to study the structure-dependent decomposition of HCOOH on Au-based bimetallic surfaces.

In this article, using first-principles approaches, the detailed reaction processes were investigated for the direct and indirect oxidation pathways of formic acid on Pd(111) and PdAu(111) surfaces. The reaction pathway HCOOH → COOH → CO is predominant on Pd(111) and Pd monolayer supported on Au(111) surface, due to the lower reaction barriers (0.50 and 0.60 eV) for the production of CO compared to the barriers (0.77 and 0.85 eV) for CO_2 formation from $HCOO_{ad}$ in direct pathway. Importantly, the production of CO for HCOOH's decomposition can be reduced on Pd-decorated Au(111) surfaces with high barriers (~1.00 eV). Our results indicate the particular importance of the ensemble effects to tune the activity and selectivity of PdAu bimetallic surfaces for the oxidation of formic acid.

2. Computational details

Our calculations were performed in the framework of the density functional theory (DFT), implemented in the plane-wave based Vienna ab initio Simulation Package (VASP) [27,28]. The interaction between ion and core electrons is described by the projector augmented wave (PAW) method [29], and plane waves with an energy cutoff of 400 eV are used to expand the Kohn-Sham (KS) wave functions. The generalized gradient approximation (GGA) for the exchange and correlation functional is employed with Perdew–Burke–Ernzerhof (PBE) scheme [30]. For the adsorbates with open-shell configuration, the spin-polarized calculations were performed. The Pd(111) and Au(111) surfaces are modeled using four (111) layers with a 15 Å vacuum in the z direction to separate the slabs, and a p(3×3) supercell with nine atoms at each layer is used in the lateral plane, which is constructed by fcc lattice with the calculated lattice constants of 4.18 and 3.96 Å for Au and Pd bulk, respectively. The gold atoms on the outmost layer are replaced by Pd atoms to construct different geometrical distributions on AuPd bimetallic surface (see Fig. 1). We select three PdAu(111) surfaces, that is, Pd monolayer supported on Au(111) (i.e., Pd ML), and Pd-decorated Au(111) surfaces (i.e., Pd_6Au_3 and Pd_3Au_6). In the calculations, the integrals in the reciprocal space are evaluated through summations over $5 \times 5 \times 1$ k points in the Monkhorst-Pack grids [31], and the positions of all atoms except those in the two bottommost layers are fully relaxed according to the calculated atomic forces (less than 0.03 eV $Å^{-1}$).

The transition states (TS) and detailed minimum-energy pathways (MEPs) for HCOOH's dehydrogenation on metal surfaces were obtained using the Climbing Image Nudged Elastic Band (CI-NEB) technique [32–35] combined with dimer method [36]. In the dimer method, a more reliable transition state was confirmed from adsorption state and saddle point guessed by NEB simulations, and the tolerance for convergence to the transition state is such that the force on each atom is less than 0.005 eV $Å^{-1}$. All transition states were confirmed using a finite-difference normal mode analysis, and only one imaginary frequency was obtained at each TS. In the calculations of the Hessian matrix, only the degrees of freedom of the adsorbates are included. The barrier (E_a) and reaction energy (ΔE) are calculated by $E_a = E_{TS} - E_{IS}$ and $\Delta E = E_{FS} - E_{IS}$, where E_{IS}, E_{TS}, and E_{FS} are the total energies of the initial state (IS), transition state (TS), and final state (FS), respectively.

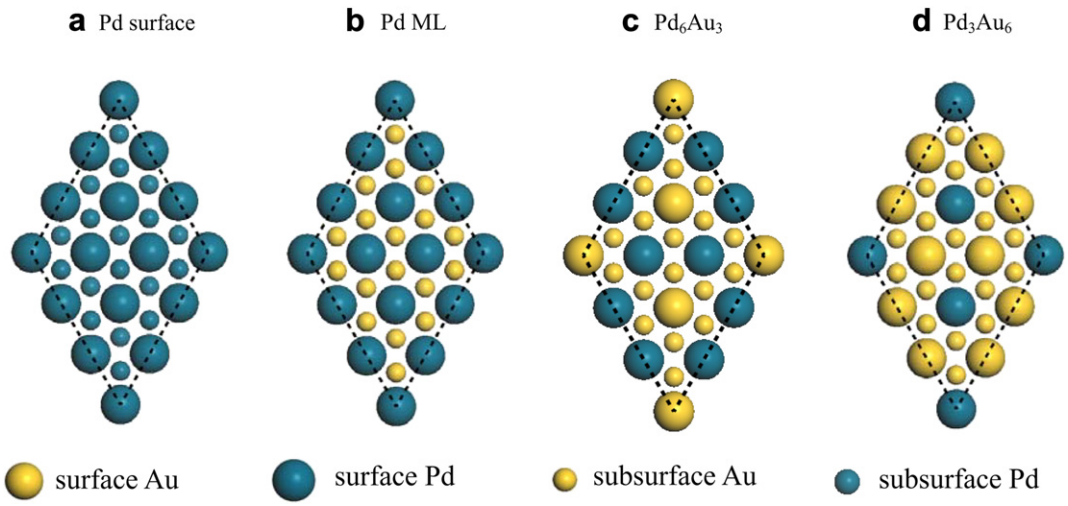

Fig. 1. The unit cells and distribution of different Pd ensembles incorporated into Au(111) surface. The dotted lines are the boundaries of unit cells used in our calculations.

3. Results and discussion

3.1. Adsorption of HCOOH, HCOO, and COOH

In order to understand the reaction pathways of HCOOH's decomposition, we first calculated the most stable adsorption configurations of the main reaction intermediates. The most stable geometrical configurations and adsorption energies are presented in Fig. 2. The adsorption energies are calculated by the total energy differences between the related systems as $E_{ad} = E_{adsorbate/substrate} - E_{substrate} - E_{adsorbate}$. Formic acid weakly binds to a Pd atop site of surface through the carbonyl oxygen attributed to its close-shell electronic configuration, and the H atom of OH group points towards the surface with an elongated O–H bond, which is 0.03–0.04 Å longer than that (0.983 Å) in gas formic acid (see Fig. 2). It should be noted that the adsorption energy of HCOOH is about −0.40 eV, which is almost unchangeable from Pd surface to the isolated Pd monomer incorporated into Au(111).The O–Pd bond lengths also remain very close to each other on Pd(111) and PdAu(111) surfaces (see Fig. 2). The adsorption energy and geometrical configuration are similar to the reported results for HCOOH's adsorption on Pt(111), Pd(111) and Ni(111) surfaces [8,9,37].

Experimental investigations confirmed the adsorbed formate ($HCOO_{ad}$) is a reactive intermediate in the direct pathway of formic acid oxidation, which is formed through the O–H bond cleavage of $HCOOH_{ad}$. [7] The bridge-bonded formate shows high stability with a much larger adsorption of −2.60 ∼ −2.10 eV resulted from its open-shell configuration. The O–Pd bond lengths are slightly shorter than these in $HCOOH_{ad}$ (see Fig. 2). The stable bidentate bridge configuration in a di-σ mode were also found on other metal catalysts (e.g., Cu(111), Pt(111), Ag–Pd core–shell nanoparticle, and Pt-decorated Au(100)) by theoretical and experimental investigations [4,8,9,38,39]. Notably, the adsorption energy of HCOO is closely related to the geometrical arrangements of Pd atoms. On Pd monomer, HCOO adsorbs on the Au–Pd bridge site, and then its adsorption energy is reduced to −2.10 eV due to the weak interaction between Au and O. In this adsorption configuration, the activation of HCOO's C–H bond should require a higher barrier (>1.00 eV), which is the rate-limiting step for the directed oxidation of formic acid on Pt surface [21,37].

Another intermediate, hydroxycarbonyl (COOH), is formed by the scission of C–H bond during the dehydrogenation process of $HCOOH_{ad}$. COOH adsorbs on the atop sites of Pd atoms through its carbon and oxygen on Pd(111), Pd monolayer, and Pd_6Au_3 surfaces, and its H atom tilts downward towards the surfaces. The unsaturated carbon of $COOH_{ad}$ also results in a high adsorption energy with −2.36 eV on Pd(111) surface, and the Pd–O and Pd–C distances are 2.235 and 1.970 Å, respectively. The Pd distribution on Au(111) surface also affects the stability and geometry of $COOH_{ad}$, and a weaker interaction is found on Pd monolayer and Pd_6Au_3 surfaces with the adsorption energies of −2.28 and −2.10 eV, respectively. In comparison with the contiguous Pd ensembles, COOH binds to the isolated Pd monomer only through the Pd–C bond due to the unavailability of the first neighboring Pd pair, and the similar adsorption configuration was reported on Pt-decorated Au(100) surface [39]. The adsorption energy of COOH is only −1.98 eV on Pd_3Au_6 surface. Consequently, the Pd–O and Pd–C bond lengths are longer for COOH's adsorption on PdAu(111) surfaces than these on Pd(111) surface (see Fig. 2).

Overall, the Pd atoms alloyed into Au(111) surface are also reactive towards the adsorption of reactants for formic acid decomposition by contrast with the pure Pd(111) surface, though the low loading of Pd on AuPd surface will reduce the binding ability. In previous calculations, we found the electronic structures, e.g., Pd-*d* band, strongly depend on the atomic arrangements of Pd ensembles on PdAu surfaces, and a narrowing *d*-band is shown for the isolated Pd ensembles incorporated into Au(111). [40] However, in present calculations, the similar mechanism is shown for HCOOH's adsorption on the contiguous and isolated Pd ensembles, namely donation and back-donation interaction between the Pd d-orbital and the lone pair orbital of oxygen of HCOOH (see Fig. 3). Charge depletion occurs on p_z and d_{z^2}. But, charge accumulation is found on the d_{xz} and d_{yz} orbitals of Pd and the p_x and p_y orbitals of oxygen. The OH group of HCOOH point towards the metal surfaces, and the Pd–H interaction results in a charge accumulation in Pd–H bond. This bonding mechanism is similar to the interaction between water and metal surface [41]. From the projected density of states (PDOS), the adsorbed formic acid holds the evident molecular orbital's characters (see Fig. 3), and the properties of Pd-d's bands of surfaces play a negligible role for HCOOH's adsorption. In general, the adsorbate–metal interactions for the molecule with a lone-pair character lead to rather weak adsorption. For HCOO and COOH, strong chemical bonds are formed between adsorbates and surfaces, and the bond formation can be described in terms of the Newns–Anderson model [42,43]. The hybridization of the localized molecular orbitals with the extended d bands of metals results in a strong covalent bonding between adsorbates and substrates. For instance, there is an extended O-2p character in the Pd-d's band region for HCOO's adsorption, which indicates a covalent contribution (see Fig. 4). The charge density difference plots show the charge accumulation into the Pd–O and Au–O bond region. For COOH, the hybridization is mainly attributed to C-p and Pd-d, and an evident charge accumulation is found in Pd–C bond (see Fig. 5). On isolated Pd atom, notably, the narrower Pd-d band leads to a weaker interaction between O(or C)-p and Pd-d for HCOO, and COOH as well.

3.2. Non-CO pathway

As mentioned above, the dual pathways of HCOOH's decomposition start from the O–H and C–H bond scission for the direct and indirect pathways, respectively. In the direct pathways, the H production is fulfilled through CO-free pathways. In our calculations, the non-CO pathway of HCOOH's dehydrogenation is described by HCOOH → HCOO → CO_2. The energies and geometries of transition states are summarized in Fig. 6 for this reaction pathway.

Experimentally, it was confirmed that formate is the stable intermediate for the decomposition of formic acid [7]. Here, we find the H atom of OH group can be easily removed with a low barrier (0.49 and 0.44 eV) for Pd(111) and Pd monolayer supported on Au(111). During the process of the O–H bond scission, the H atom binds to the Pd bridge site, and the bond length of Pd–H is ∼1.80 Å in transition state on Pd(111) and Pd monolayer. However, on Pd_6Au_3 and Pd_3Au_6 surfaces, the Au atoms adjacent to Pd sites evidently enhance the activation barrier for the reaction HCOOH → HCOO + H, and barriers are 0.71 and 0.96 eV, respectively. Pd bridge site isn't available for H adsorption of OH group in transition state (TS1) on Pd_6Au_3 and Pd_3Au_6 surfaces, and the H binds to Pd–Au or Au–Au bridge with the bond lengths ranging from 1.780 to 1.825 Å. Thus, the contiguous Pd ensemble is favorable for breaking the O–H bond of $HCOOH_{ad}$ on PdAu electrode during formic acid electro-oxidation. In TS1, the interaction of O–H bond is very weak, and the O–H bond lengths are markedly stretched to 1.619–1.813 Å. On Pd(111) and Pd ML, H binds to Pd threefold hollow sites in final state (FS), and the reaction HCOOH → HCOO + H is exothermic with reaction energies (ΔE) of −0.09 and −0.19 eV, respectively. However, on Pd-decorated Au(111), especially Pd_3Au_6 surface, the O–H bond scission is energetically unfavorable due to the lower reactivity for the adsorption

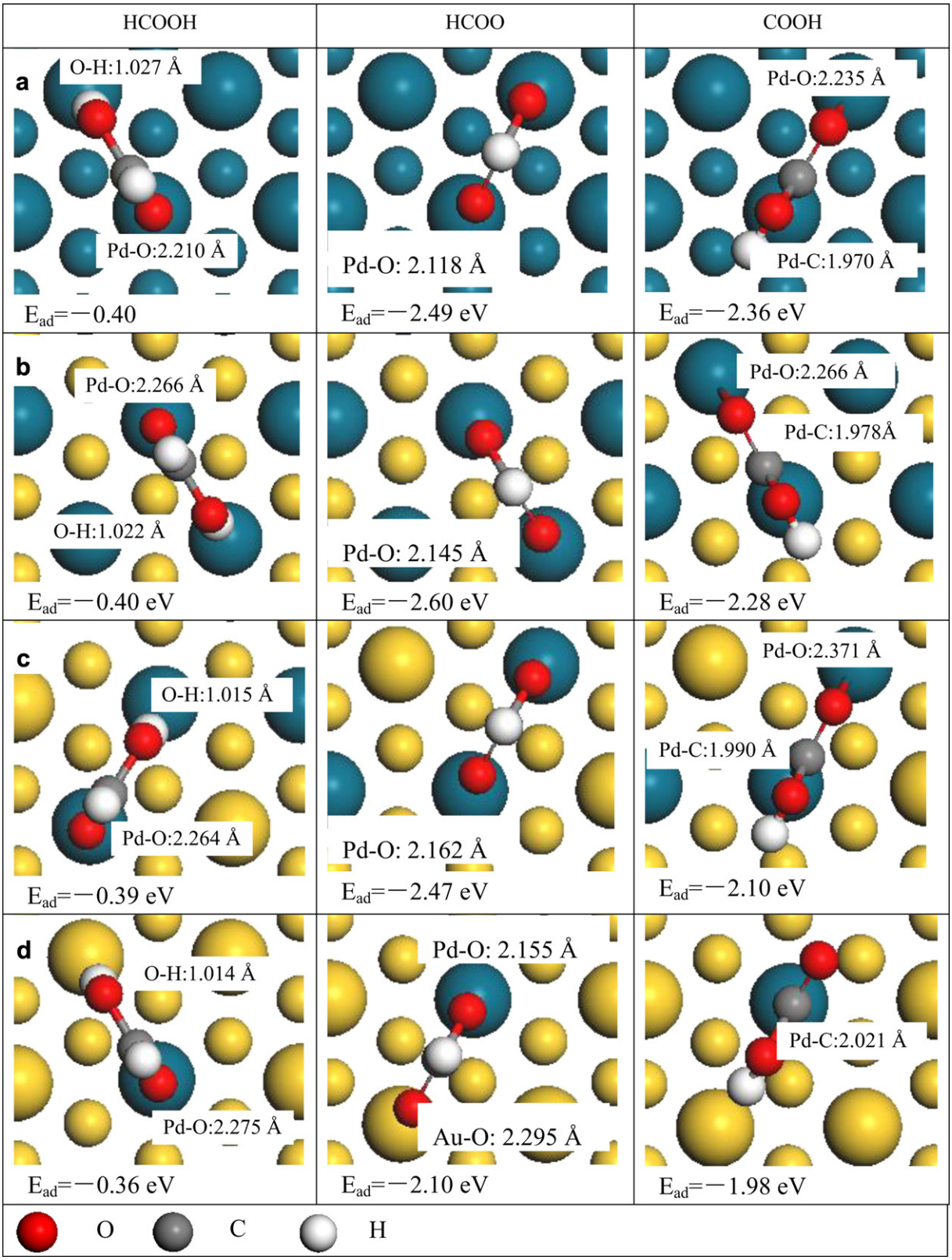

Fig. 2. The optimized adsorption geometries of different molecules, i.e., HCOOH, HCOO, and COOH, on Pd(111) surface (a), Pd ML (b), Pd_6Au_3 (c), and Pd_3Au_6 (d). The calculated adsorption energies (E_{ad}) and selected bond lengths are also presented.

of formate and H in FS. Though Pd-decorated Au(111) is less reactive than Pd(111) for the O–H bond scission of $HCOOH_{ad}$, notably, Pd ensembles incorporated into Au substrate present a similar chemical reactivity to Pt surface [8,9,37].

From the energy diagrams (Fig. 6), we can see that the second stage ($HCOO \rightarrow CO_2 + H$) is the rate-limiting step for the direct oxidation of formic acid on Pd(111) and Pd ML surfaces. A high barrier up to 1.56 eV is found on Pt(111) for the dehydrogenation of

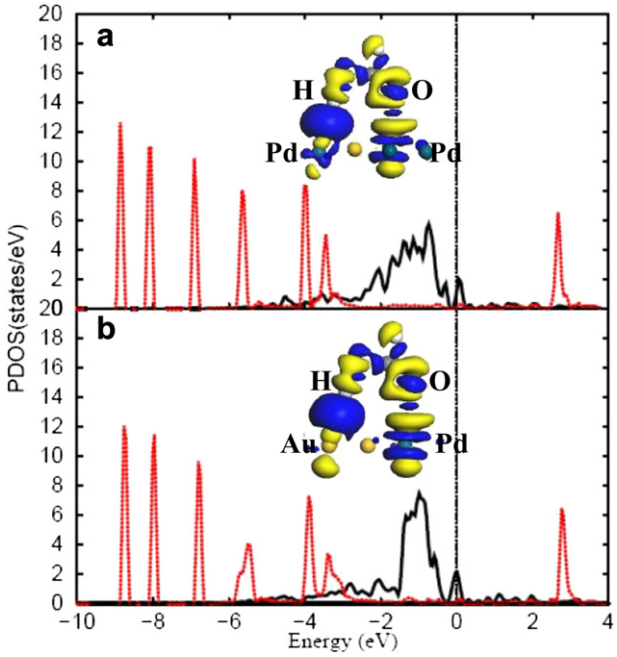

Fig. 3. The PDOS of adsorbed formic acid (red/dotted line) and Pd-d's band (black solid line) on Pd_6Au_3 (in panel a) and Pd_3Au_6 (in panel b). The inset shows the charge redistribution with the difference of charge density $\Delta\rho = \rho_{HCOOH/PdAu(111)} - \rho_{HCOOH} - \rho_{PdAu(111)}$. The blue and yellow regions represent charge accumulation and depletion, respectively. (For interpretation of the references to colour in this figure legend, the reader is referred to the web version of this article.)

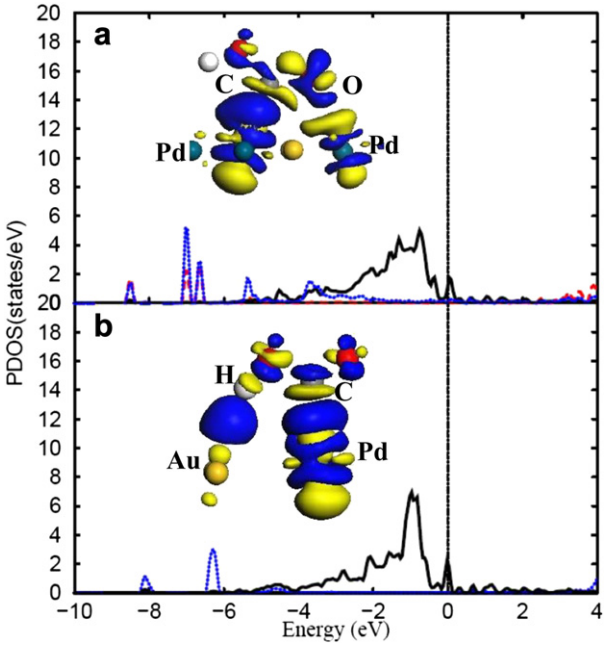

Fig. 5. The PDOS of O-p's (red/dashed line) or C-p's (blue/dotted line) orbitals in the adsorbed hydroxycarbonyl (COOH) and Pd-d's band (black solid line) on Pd_6Au_3 (in panel a) and Pd_3Au_6 (in panel b). The inset shows the charge redistribution with the difference of charge density $\Delta\rho = \rho_{COOH/PdAu(111)} - \rho_{COOH} - \rho_{PdAu(111)}$. The blue and yellow regions represent charge accumulation and depletion, respectively. (For interpretation of the references to colour in this figure legend, the reader is referred to the web version of this article.)

formate [37]. Our calculations indicate that the formate is bound to a bridge site in a di-σ mode through its two oxygen atoms with a high adsorption energy on Pd(111) and PdAu(111) surfaces. Moreover, the C–H of $HCOO_{ad}$ is oriented along the surface normal. Then, the dissociation of the C–H bond from $HCOO_{ad}$ requires significantly adjusting the molecular structure, and the molecule binds to surface's atoms through a oxygen and hydrogen in TS2 (see Fig. 6). Our calculated dehydrogenation barrier of $HCOO_{ad}$ is larger than 0.7 eV on Pd(111) and Pd-decorated Au(111) surfaces. The ensemble requirement for formate dehydrogenation is two metal atoms. Then, Pd_6Au_3 shows a similar reactivity to Pd(111) and Pd ML for CO_2 formation from $HCOO_{ad}$. On Pd(111), the barrier of HCOO → CO_2 + H is 0.77 eV, which is very agreement with the reported result (0.76 eV) [37]. Though Pd monomer presents the most higher barrier for the O–H scission of HCOOH, a lower barrier (0.72 eV) is found for HCOO's dehydrogenation, which is originated from the weaker Au–O bond in the IS. Compared with Pt surface, to some extent, the lower activation barriers can effectively avoid the site-blocking effects of formate on Pd-based catalysts in the direct pathway of formic acid oxidation [14]. In the final states, the CO_2 molecule desorbs from the surfaces, and the H atom adsorbs on the hollow site. The reaction of HCOO → CO_2 + H is exothermic with a reaction energy of −0.22 to −0.48 eV on Pd(111) and PdAu(111) surfaces.

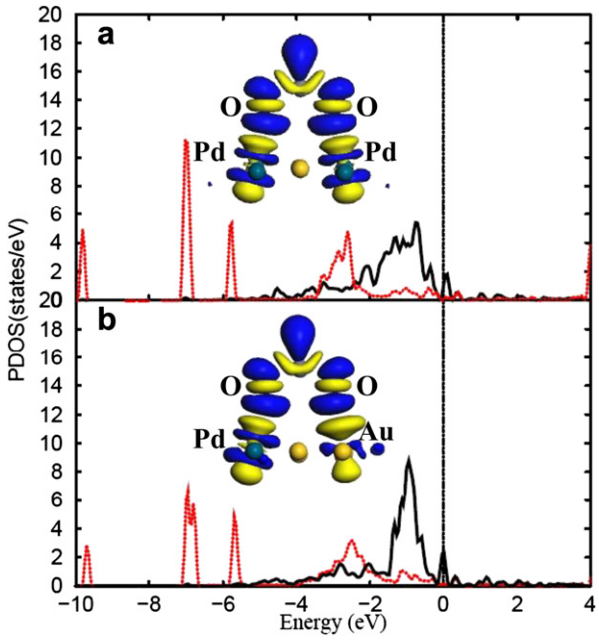

Fig. 4. The PDOS of O-p's orbitals in the adsorbed formate (red/dotted line) and Pd-*d*'s band (black solid line) on Pd_6Au_3 (in panel a) and Pd_3Au_6 (in panel b). The inset shows the charge redistribution with the difference of charge density $\Delta\rho = \rho_{HCOO/PdAu(111)} - \rho_{HCOO} - \rho_{PdAu(111)}$. The blue and yellow regions represent charge accumulation and depletion, respectively. (For interpretation of the references to colour in this figure legend, the reader is referred to the web version of this article.)

3.3. CO pathway

As shown in Fig. 7, we present the energies and geometries for formic acid oxidation on Pd(111) and PdAu(111) surfaces along the CO pathway HCOOH → COOH → CO. Also, the activation of the C–H bond of formic acid can readily occur on Pd(111) and Pd ML, and the barriers for C–H bond scission are 0.56 and 0.47 eV, respectively. In transition state (TS3), a strong Pd–C bond is formed with a bond length of 2.096–2.184 Å, and the breaking C–H bond is 1.287–1.495 Å, which is longer than that (1.106 Å) in HCOOH molecule. Moreover, on contiguous Pd ensembles (i.e., Pd(111), Pd ML, and Pd_6Au_3 surfaces), formic acid binds to three substrate's atoms through Pd–C, Pd–O, and Pd–H (or Au–H) bonds in TS3.

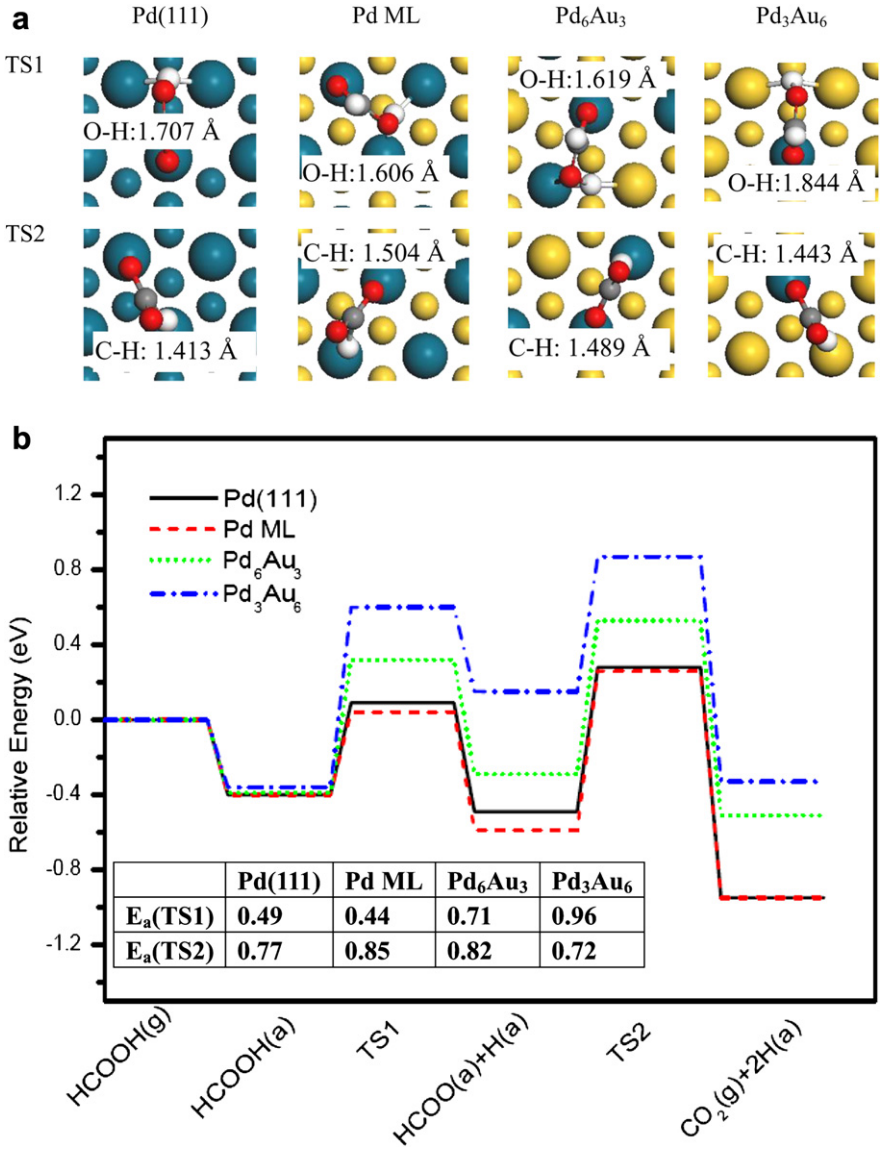

	Pd(111)	Pd ML	Pd_6Au_3	Pd_3Au_6
E_a(TS1)	0.49	0.44	0.71	0.96
E_a(TS2)	0.77	0.85	0.82	0.72

Fig. 6. In panel a: the calculated geometries of transition states (TS1 and TS2) and the breaking O—H (in TS1) and C—H (in TS2) bond lengths. In panel b: energies (in eV) of formic acid oxidation along the non-CO pathway HCOOH → HCOO → CO_2 on Pd(111) surface (black solid line) and PdAu(111) surfaces, i.e., Pd ML (red/dashed line), Pd_6Au_3 (green/dotted line), and Pd_3Au_6 (blue/dashed and dotted line). The energy barriers (E_a) are inserted in eV. (For interpretation of the references to colour in this figure legend, the reader is referred to the web version of this article.)

However, on Pd monomer ensemble, Pd—O bond is broken during the formation of COOH from HCOOH's dehydrogenation, and formic acid prefers to be adsorbed at two metal atoms through Pd—C, Pd—H, and Au—H bonds in TS3. On Pd_6Au_3 and Pd_3Au_6 surfaces, only Pd—Au bridge site is available for H adsorption in transition state, and the barriers for C—H bond cleavage are increased to 0.72 and 0.75 eV, respectively. By comparison, these barriers are substantially lower than that (1.58 eV) found on Pt(111) for breaking C—H of $HCOOH_{ad}$. [8] Due to the "ligand effect", PdAu(111) surfaces show low reactivity for the adsorption of COOH and H in FS, which results in the process of C—H scission is also endothermic with the reaction energies of 0.22 and 0.39 eV on Pd_6Au_3 and Pd_3Au_6 surfaces, respectively. The adsorption of intermediates for HCOOH's decomposition requires only a single or two active metal atoms [21]. In the initial state, the adsorption of formic acid only require a single Pd atom, and the geometrical distribution of Pd atom on Au(111) play a negligible influence on the stability of $HCOOH_{ad}$. However, the activation of the O—H and C—H bond of formic acid involve a larger atomic ensemble, and three first-neighbor Pd atoms are favorable for stabilizing TS and FS. Notably, the isolated Pd atom incorporated into Au(111) show a very low chemical reactivity for the dehydrogenation of formic acid. Importantly, the calculations for the dehydrogenation of formic acid indicate that the C—H and O—H activation can simultaneously occur on Pd and PdAu catalysts due to their similar activation barriers. The Pd-based catalysts exhibit a high chemical reactivity for the H scission of $HCOOH_{ad}$ when compared to Pt surface.

The poisoning species of CO_{ad} is mainly produced by the decomposition of $COOH_{ad}$ in the indirect path. In the second step of indirect pathway for the HCOOH's oxidation, we consider the reaction of COOH → CO + OH (shown in Fig. 7). Interestingly, the activation energy breaking C—O bond of $COOH_{ad}$ strongly depends on the atomic distribution of PdAu surfaces. On Pd ML, the CO formation proceeds with a barrier of only 0.50 eV, which is similar to the activation energy (0.60 eV) on Pd(111). The C—O dissociation of $COOH_{ad}$ is exothermic with the reaction energies of −0.52

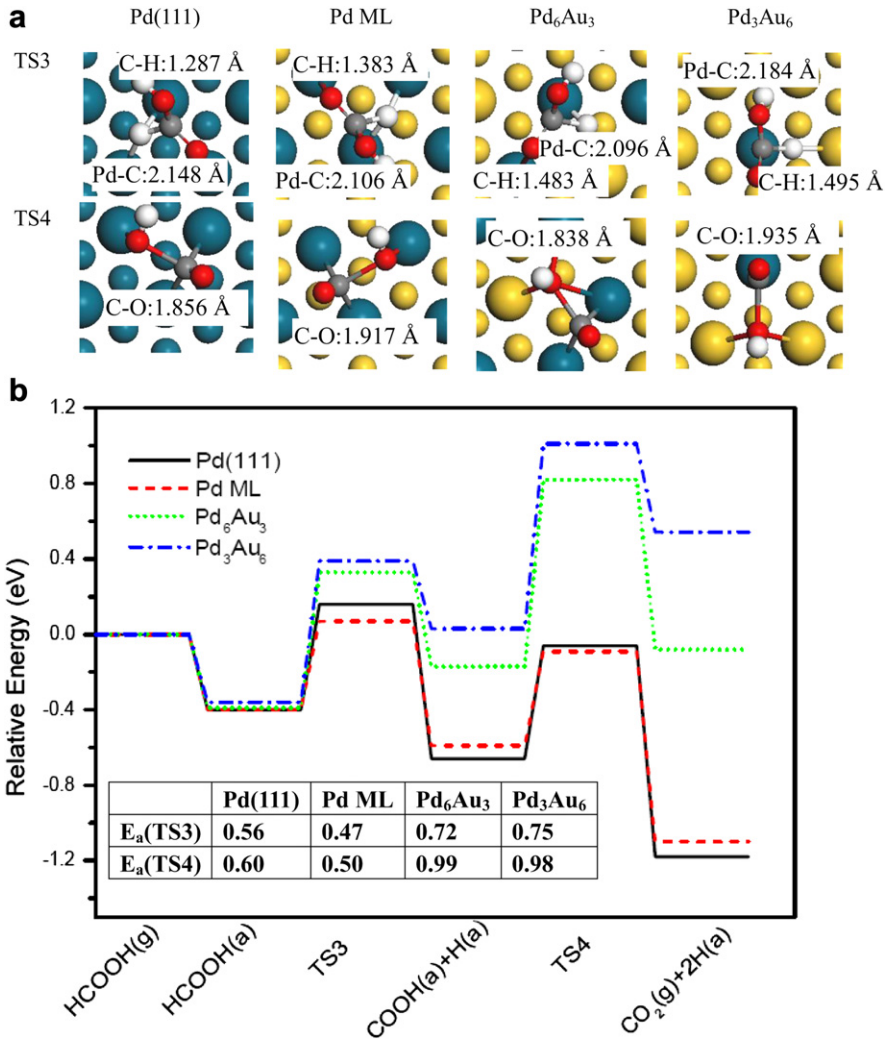

	Pd(111)	Pd ML	Pd_6Au_3	Pd_3Au_6
E_a(TS3)	0.56	0.47	0.72	0.75
E_a(TS4)	0.60	0.50	0.99	0.98

Fig. 7. In panel a: the calculated geometries of transition states (TS3 and TS4) and the breaking C—H (in TS3) and C—O (in TS4) bond lengths. In panel b: energies (in eV) of formic acid oxidation along the CO pathway HCOOH → COOH → CO on Pd(111) surface (black solid line) and PdAu(111) surfaces, i.e., Pd ML (red/dashed line), Pd_6Au_3 (green/dotted line), and Pd_3Au_6 (blue/dashed and dotted line). The energy barriers (E_a) are inserted in eV. (For interpretation of the references to colour in this figure legend, the reader is referred to the web version of this article.)

and −0.51 eV on Pd(111) and Pd ML, respectively, and the final products (OH and CO) bind to the Pd threefold hollow sites. A sizable energy barrier (∼1.00 eV) for CO formation is found on Pd_6Au_3 and Pd_3Au_6 surfaces. Particularly, the reaction of COOH → CO + OH is highly energetically unfavorable on Pd monomer, and the reaction energy is 0.51 eV, indicating an endothermic process. In transition state (TS4), three contiguous Pd atoms are involved for stabilizing two segments (CO and OH) of COOH on Pd(111) and Pd ML, and they bind to the Pd bridge and top site, respectively. On Pd_6Au_3 surface, OH group approach to Au—Pd—Pd hollow site, and CO group still binds to Pd bridge site in TS4. Due to the geometrical effect, Pd—O bond lengths are ∼2.66 Å, and the interaction is very weak between OH group and Pd_6Au_3 surface in TS4. On Pd_3Au_6 surface, Pd monomer is less active for molecular adsorption state of COOH and transition state (TS4) in the reaction of COOH → CO + OH. Specifically, CO group binds to the top site of the isolated Pd atom, and OH group adsorbs at the Au—Au bridge site in TS4. At the transition states (TS4), the C—O bond is already broken, and the distance between C and O is 1.838—1.935 Å on the Pd(111) and PdAu(111) surfaces. Overall, on the PdAu(111) surface without such atomic ensembles consisting of three continuous Pd atoms, the formation rate of CO can be significantly reduced during the processes of formic acid oxidation.

3.4. COOH dehydrogenation

The adsorbed COOH can also decompose into an adsorbed H atom and a gas phase CO_2 molecule (see Fig. 8). In the transition states (TS5), the OCO fragment binds to the Pd top site through C atom with a O=C=O angle of ∼140° on Pd(111) and PdAu(111) surfaces, and the O—H bond is elongated to 1.435—1.512 Å. On Pd(111) and Pd ML, the Pd—Pd bridge is available for H adsorption in TS5. However, only two metal atoms are involved for breaking O—H bond of $COOH_{ad}$ on Pd_6Au_3 and Pd_3Au_6 surfaces, and H atom approaches to Pd or Au top site. Notably, for COOH → CO_2 + H, the activation energies (0.80 and 0.75 eV) are higher than these (0.60 and 0.50 eV) for COOH → CO + OH on Pd(111) and Pd ML. Contrarily, CO_2 formation shows lower barriers (0.84 and 0.87 eV) than these (0.99 and 0.98 eV) of CO production from $COOH_{ad}$ on Pd_6Au_3 and Pd_3Au_6 surfaces, which provides a good chance for CO-free production of H_2 from formic acid. The reaction of

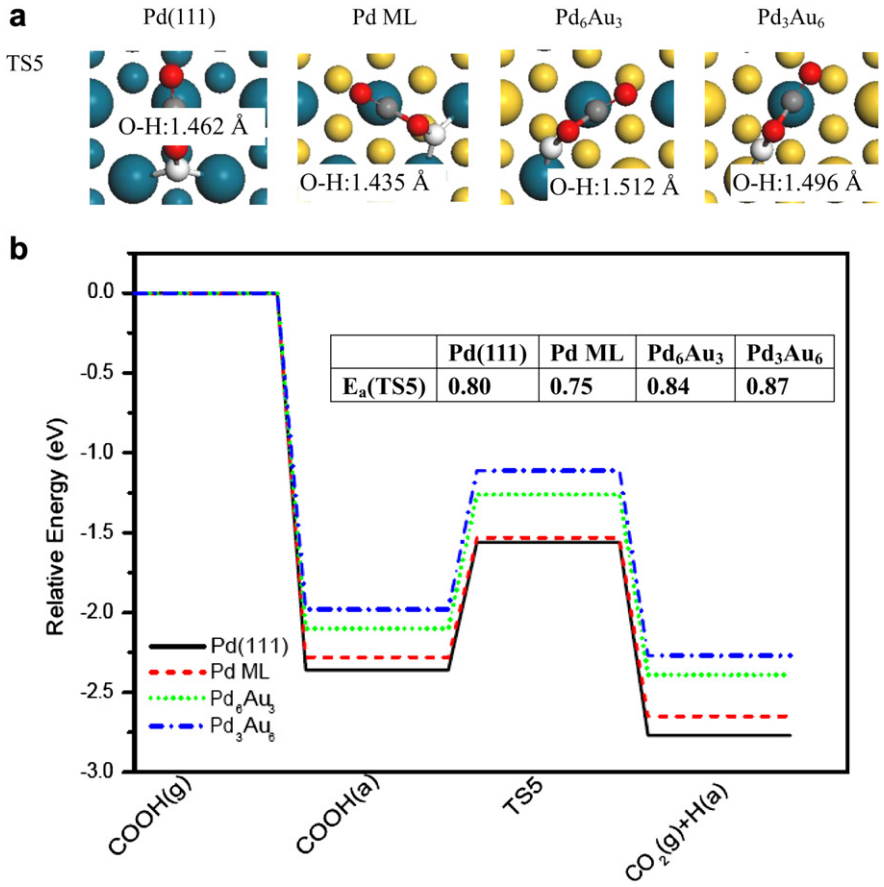

Fig. 8. In panel a: the calculated geometries of transition state (TS5) and the breaking O–H (in TS5) bond lengths. In panel b: energies (in eV) of COOH's dehydrogenation on Pd(111) surface (black solid line) and PdAu(111) surfaces, i.e., Pd ML (red/dashed line), Pd_6Au_3 (green/dotted line), and Pd_3Au_6 (blue/dashed and dotted line). The energy barriers (E_a) are inserted in eV. (For interpretation of the references to colour in this figure legend, the reader is referred to the web version of this article.)

COOH → CO_2 + H is exothermic with a reaction energy of −0.29 to −0.41 eV on Pd(111) and PdAu(111) surfaces.

3.5. Ensemble effects on HCOOH decomposition

As known, the activation energy of molecular decomposition relies on the stability of two segments in the transition state. Hence the dissociative barrier (E_a) is more sensitive to the atomic distribution of alloy surface, namely, the ensemble effects [22]. M. Neurock et al. suggested a unique active atomic ensemble is required for the different reaction stages and pathways of the catalytic oxidation of methanol and formic acid on Pt-based catalysts [21]. Our previous calculations also indicated that a proper arrangement of Au and Pt sites can offer great opportunities for non-CO_{ad} paths for high H productivity in the direct methanol fuel cells [22]. The reaction pathways of formic acid oxidation are schematically shown in Fig. 9. The poisoning species of CO_{ad} are formed by COOH's decomposition, but CO_2 formation proceeds through both C–H and O–H activation. Our calculations indicate that the catalytic activity and selectivity of PdAu(111) surface towards formic acid decomposition are markedly dependent on the atomic geometrical distribution of reaction sites. In these pathways, the reactions HCOOH → HCOO + H, HCOOH → COOH + H, and COOH → CO + OH require three contiguous Pd atoms for reducing the barriers. Particularly, the small Pd ensembles (i.e., 1–2 Pd atoms) significantly enhance the activation energy of CO formation from the adsorbed COOH on PdAu(111) surfaces, which may facilitate the direct oxidation of formic acid through a non-CO pathway. It should be noted that the atomic arrangement of Au and Pd play only a minor role for CO_2 formation from the adsorbed HCOO and COOH. Overall, the Pd-decorated Au(111) surface with the reduction of contiguous Pd sites is highly efficient for direct formic acid oxidation, which can suppress the formation of poisonous species CO_{ad} *via* the atomic ensemble effects.

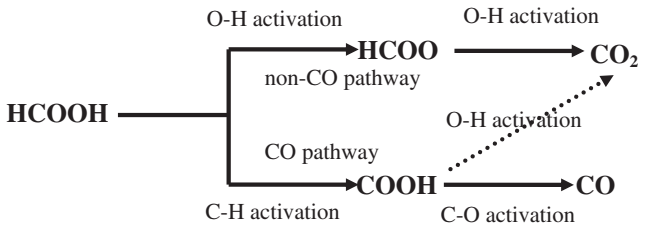

Fig. 9. Schematic diagram of the reaction pathways for formic acid decomposition.

4. Summary

Using the DFT calculations, we found that Pd-decorated Au(111) is active to catalyze the decomposition of formic acid. The adsorption energy of formic acid is very close on different Pd ensembles, but the activation of O–H and C–H bonds is related to the atomic arrangement of Au and Pd. On the contiguous ensembles without threefold Pd site, the reaction of COOH → CO + OH proceeds with a high activation energy (~1.00 eV), and the non-CO pathway is predominant for H production from formic acid.

Consequently, the ensemble effects play a crucial role to tune the reactivity and selectivity of anode catalyst in fuel cells, which originates the drastically different activities of Au and Pd sites. To design highly efficient anode catalysts of DFAFC, more extensive experimental and theoretical studies are needed for understanding the atomic-structure-dependent electrocatalytic activity of Au-based bimetallic catalysts in the oxidation process of formic acid.

Acknowledgment

This work was supported by the National Natural Science Foundation of China (Grant no. 10904034), PhD Programs Foundation of China (No. 200805321058), the National Basic Research (973) Program of China (No. 2009CB623704), and the development plan for young teacher of HuNan University. Part of calculations were performed at the Center for Computational Science of CASHIPS.

References

[1] R. Larsen, S. Ha, J. Zakzeski, R.I. Masel, J. Power Sources 157 (2006) 78.
[2] X.W. Yu, P.G. Pickup, J. Power Sources 182 (2008) 124.
[3] K. Tedsree, T. Li, S. Jones, C.W.A. Chan, K.M.K. Yu, P.A.J. Bagot, E.A. Marquis, G.D.W. Smith, S.C.E. Tsang, Nat. Nanotechnol. 6 (2011) 302.
[4] A. Wittstock, V. Zielasek, J. Biener, C.M. Friend, M. Bäumer, Science 327 (2010) 319.
[5] M. Ojeda, E. Iglesia, Angew. Chem. Int. Ed. 48 (2009) 4800.
[6] A. Gazsi, T. Bansagi, F. Solymosi, J. Phys. Chem. C 115 (2011) 15459.
[7] M. Osawa, K. Komatsu, G. Samjeské, T. Uchida, t. Ikeshoji, A. Cuesta, C. Gutiérrz, Angew. Chem. Int. Ed. 50 (2011) 1159.
[8] W. Gao, J.A. Keith, J. Anton, T. Jacob, Dalton Trans. 39 (2010) 8450.
[9] W. Gao, J.A. Keith, J. Anton, T. Jacob, J. Am. Chem. Soc. 132 (2010) 18377.
[10] N. Kristian, Y.S. Yan, X. Wang, Chem. Commun. 3 (2008) 353.
[11] I.S. Park, K.S. Lee, J.H. Choi, H.Y. Park, Y.E. Sung, J. Phys. Chem. C 111 (2007) 19126.
[12] M.D. Obradović, A.V. Tripković, S.L. Gojković, Electrochim. Acta 55 (2009) 204.
[13] W.J. Zhou, J.Y. Lee, J. Phys. Chem. C 112 (2008) 3789.
[14] J.W. Hong, D. Kim, Y.W. Lee, M. Kim, S.W. Kang, S.W. Han, Angew. Chem. Int. Ed. 50 (2011) 8876.
[15] X.J. Gu, Z.H. Lu, H.L. Jiang, T. Akita, Q. Xu, J. Am. Chem. Soc. 133 (2011) 11822.
[16] Y. Liu, L.W. Wang, G. Wang, C. Deng, B. Wu, Y. Gao, J. Phys. Chem. C 114 (2010) 21417.
[17] J.A. Rodriguez, D.W. Goodman, Science 257 (1992) 897.
[18] J.R. Kitchin, J.K. Nørskov, M.A. Barteau, J.G. Chen, Phys. Rev. Lett. 93 (1992) 156801 (2004).
[19] J.A. Rodriguez, Surf. Sci. Rep. 24 (1996) 225.
[20] F. Maroun, F. Ozanam, O.M. Magnussen, R.J. Behm, Science 293 (2001) 1811.
[21] M. Neurock, M. Janik, A. Wieckowski, Faraday Discuss. 140 (2008) 363.
[22] D.W. Yuan, X.G. Gong, R.W. Wu, J. Chem. Phys. 128 (2008) 064706.
[23] D.W. Yuan, Z.R. Liu, J.H. Chen, J. Chem. Phys. 134 (2011) 054704.
[24] M.S. Chen, D. Kumar, C.W. Yi, D.W. Goodman, Science 310 (2005) 291.
[25] D.W. Yuan, X.G. Gong, R.Q. Wu, J. Phys. Chem. C 112 (2008) 1539.
[26] F. Gao, Y.L. Wang, D.W. Goodman, J. Am. Chem. Soc. 131 (2009) 5734.
[27] G. Kresse, J. Furthmuller, Phys. Rev. B 54 (1996) 11169.
[28] G. Kresse, J. Furthmuller, Comput. Mater. Sci. 6 (1996) 15.
[29] G. Kresse, D. Joubert, Phys. Rev. B 59 (1999) 1758.
[30] J.P. Perdew, K. Burke, M. Ernzerhof, Phys. Rev. Lett. 77 (1996) 3865.
[31] H.J. Monkhorst, J.D. Pack, Phys. Rev. B 13 (1976) 5188.
[32] G. Schenter, G. Mills, H. Jónsson, J. Chem. Phys. 101 (1994) 8964.
[33] G. Mills, H. Jónsson, G. Schenter, Surf. Sci. 324 (1995) 305.
[34] G. Henkelman, H. Jónsson, J. Chem. Phys. 113 (2000) 9978.
[35] G. Henkelman, B.P. Uberuaga, H. Jónsson, J. Chem. Phys. 113 (2000) 9901.
[36] G. Henkelmana, H. Jónsson, J. Chem. Phys. 111 (1999) 7010.
[37] Q.Q. Luo, G. Feng, M. Beller, H.J. Jiao, J. Phys. Chem. C 116 (2012) 4149.
[38] Z.M. Hu, R.J. Boyd, J. Phys. Chem. 112 (2000) 9562.
[39] Y.L. Yu, X. Wang, K.H. Lim, Catal. Lett. 141 (2011) 1872.
[40] D.W. Yuan, X.G. Gong, R.Q. Wu, Phys. Rev. B 75 (2007) 085428.
[41] H. Ogasawara, B. Brena, D. Nordlund, M. Nyberg, A. Pelmenschikov, L.G.M. Pettersson, A. Nilsson, Phys. Rev. Lett. 89 (2002) 276102.
[42] P.W. Anderson, Phys. Rev. 124 (1961) 41.
[43] D.M. Newns, Phys. Rev. 178 (1969) 1123.